# Rational Optimization of the Binding Affinity of CD4 Targeting Peptidomimetics with Potential Anti HIV Activity

Axel T. Neffe,* Matthias Bilang, Ilona Grüneberg, and Bernd Meyer

*Institute for Organic Chemistry, University of Hamburg, Martin Luther King Platz 6, 20146 Hamburg, Germany*

*Received February 22, 2007*

We recently reported the design and synthesis of a CD4 binding peptidomimetic with potential as HIV entry inhibitor. Variation of side chains and amino terminus provided first structure−activity relationships and confirmed the activity of the compounds as well as the correctness of our approach [Neffe, A. T.; Bilang, M.; Meyer, B. *Org. Biomol. Chem.* **2006**, *4*, 3259−3267]. Here we describe optimizations at the carboxy terminus of the peptidomimetic CD4 ligands resulting in the highest binding affinity of $K_D = 6\ \mu M$ for compound **4** determined with surface plasmon resonance (SPR). Saturation transfer difference NMR experiments with two peptidomimetics give binding constants similar to the SPR experiments and verified the ligand binding epitope. The higher proteolytic stability of the peptidomimetics compared to the lead peptide is demonstrated in a pronase digestion assay. Comparison of modeling and analytical data shows good agreement of theoretical and practical experiments.

## Introduction

Human immunodeficiency virus (HIV) infection is treated nowadays with a combination therapy (highly active antiretroviral therapy, HAART)[1] of drugs normally belonging to one of three main antiviral drug classes, nucleosidic reverse transcriptase inhibitors (NRTIs[a]), non-nucleosidic reverse transcriptase inhibitors (nNRTIs), and protease inhibitors (PIs).[2] Despite their efficacy in suppressing HIV replication, none of these drugs nor their combination can cure HIV infection.[3] This is mainly due to the high mutation rate of HIV and the resulting resistances of HIV strains against treatment.[4] Furthermore, the mutations often lead to cross resistance of the drugs known so far.[5] New drug classes have to be developed,[6] as vaccination attempts have not been successful.[7] Each step in the viral reproduction cycle is a potential drug target.[8] Attempts for the inhibition of recognition, coreceptor binding, membrane fusion (these three steps together are referred to as entry), transcription of the viral RNA into DNA, integration, and assembly of proteins and DNA to new viral particles are the focus of research for potential anti-HIV drugs.

The 36meric peptide Ac-YTSLIHSLIEESQNQQEKNEQEL-LELDKWASLWNWF-$NH_2$ (enfuvirtide, T20) is the first approved entry inhibitor and has proved to be very useful in combination therapy.[9] However, the first HIV strains with resistance against this drug have emerged.[10] While T20 is directed against membrane fusion, earlier steps in the infection cycle are also very promising targets. The first step in the infection of a human cell with HIV is the interaction between the viral envelope glycoprotein gp120 and the human CD4.[11] Only after CD4 binding, gp120 can interact with a coreceptor,[12] normally CCR5 or CXCR4,[13] leading to gp41-mediated membrane fusion and infection of the cell.[14]

Targeting the interaction of gp120 with CD4, others developed either gp120 or antibody related peptides to bind CD4[15] or gp120 binding molecules.[16] One challenge in the development of a CD4 binding drug is to minimize the potential interference with the human immune system, as CD4 plays an important role in the binding of MHC class II proteins to T cell receptors.[17] The binding sites of CD4 to gp120 and MHC class II proteins overlap.[18] However, the contact area of the gp120 CD4 interaction is much bigger (and therefore stronger) than the CD4 MHC class II protein interaction.[19]

Viral resistance is not a major concern in the attempt of CD4 binding drugs, because this would require the virus to change its entry mechanism totally. This would only be possible in the case of multiple simultaneous mutations and is, thus, not very likely.

The peptide NMWQKVGTPL **1** binds to CD4 and shows antiviral activity in a HIV proliferation assay.[20] Starting from this peptide, we developed the peptidomimetic compound **2** (Table 1).[21] The two *N*-terminal amino acids (asparagine and methionine) of **1** do not contribute to binding and were thus removed from the lead structure. Likewise, the internal glutamine of **1** was replaced by a spacer, as it also does not contribute to binding. This results in a virtual lead structure W-spacer-KVGTPL. The two terminal hydrophobic amino acids tryptophane and leucine were replaced by generic hydrophobic residues. As a result, only four peptidic bonds were left in the molecule **2**. Ligand **2** showed an increased binding affinity to CD4 compared to the lead ($K_D = 35\ \mu M$ compared to $K_D = 6000\ \mu M$ for the decapeptide **1**), while having improved pharmacological properties (lower molecular weight, higher proteolytic stability, more suitable logP).

With the help of the saturation transfer difference (STD) NMR and modeling data,[22] we derived a series of similar compounds having single substitutions of the aromatic ring or amino acids of the core.[23] This led to compounds with $K_D$ values down to 10 $\mu$M. In this paper we focus on modifications for

* To whom correspondence should be addressed. Present address: GKSS Research Centre, Institute for Polymer Research, Kantstrasse 55, 14513 Teltow, Germany. Phone: +49-3320-352325. Fax: +49-3328-352452. E-mail: axel.neffe@gkss.de.

[a] Abbreviations: CV, column volume; DMF, dimethyl formamide; HSQC, hetero single quantum coherence; $K_D$, dissociation constant; MALDI-TOF MS, matrix-assisted laser desorption ionization time of flight mass spectrometry; nNRTI, non-nucleosidic reverse transcriptase inhibitor; NRTI, nucleosidic reverse transcriptase inhibitor; PI, protease inhibitor; ROESY, rotating frame Overhauser enhancement spectroscopy; RU, response units; SPR, surface plasmon resonance; STD, saturation transfer difference; TBTU, *O*-(benzotriazol-1-yl)-*N*,*N*,*N*′,*N*′-tetramethyluronium tetrafluoroborate; TFA, trifluoro acetic acid; TIPS, triisopropylsilane; TOCSY, total correlated spectroscopy.

10.1021/jm070206b CCC: $37.00 
Published on Web 06/28/2007

**Table 1.** Structures, $K_D$ Values Determined by SPR, and the Calculated Binding Energies to CD4 of **1**−**11**

| Compound structure | | | Compound structure | | |
|---|---|---|---|---|---|
| No. | $K_D$ [μM] | Binding score [kcal/mol] | No. | $K_D$ [μM] | Binding score [kcal/mol] |
| $NH_2$—N M W Q K V G T P L—COOH | | | 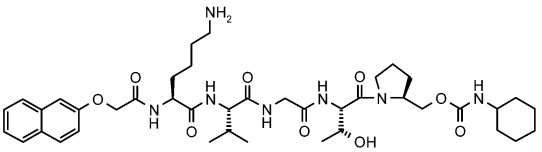 | | |
| **1** | 6000 | -321 | **2** | 35 | -376 |
| 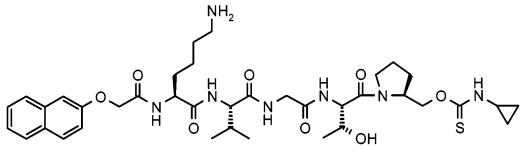 | | | 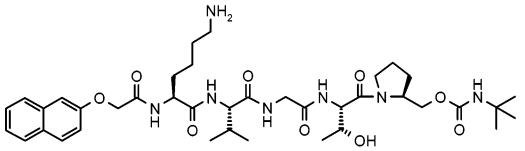 | | |
| **3** | 27 | -379 | **4** | 6 | -388 |
| 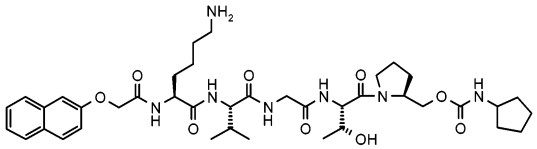 | | | 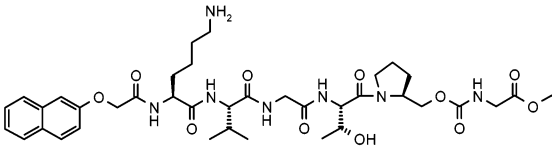 | | |
| **5** | 16 | -379 | **6** | 26 | -377 |
| 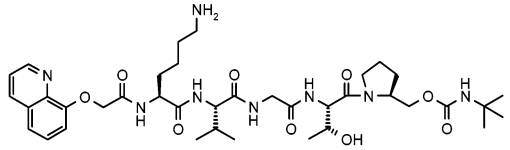 | | | 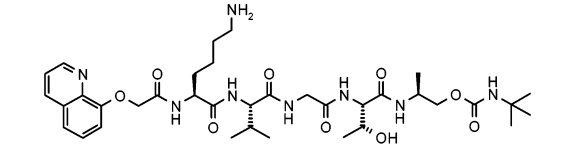 | | |
| **7** | 26 | -385 | **8** | 13 | -375 |
| 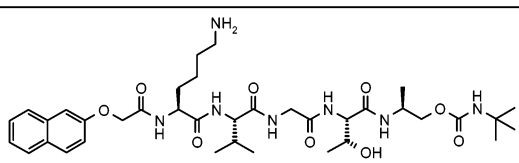 | | | 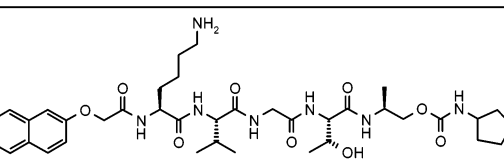 | | |
| **9** | 20 | -381 | **10** | 62 | -382 |
| 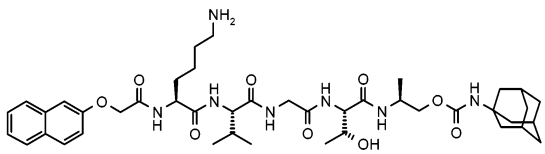 | | | | | |
| **11** | 80 | -382 | | | |

the C-terminal cyclohexyl moiety. STD NMR ligand epitope mapping showed a close contact between the cyclohexyl ring and CD4, while a compound without the cyclohexyl moiety binds ten times weaker than the corresponding peptidomimetic. This shows the carboxy terminal subunit to be essential for binding. We show the relationship of binding affinity and the carboxy terminal group and analyze the correlation of calculated and analytical results.

## Results and Discussion

We developed analogs of **2** with "carboxy terminal" hydrophobic cyclopropyl, *tert*-butyl, and cyclopentyl residues (compounds **3**−**5**, Table 1) and the ethoxy carbonyl methyl residue (**6**, Table 1). Compounds **7**−**11** (Table 1) combine subunits, which were demonstrated to improve binding to CD4.[23] Table 1 summarizes the structures, binding affinities determined by surface plasmon resonance (SPR), and the calculated binding affinities from docking experiments with Flexidock (Tripos).[24]

Syntheses were carried out, as described earlier,[21] by amide bond formation in solid phase supported reaction cycles, cleavage of the alcohol from the resin while retaining the side chain protecting groups, and subsequent carbamate bond formation under Cu(I) catalysis. The solid-phase synthesis of **3**−**11** gave yields for the unpurified primary alcohol of 32−35% (equivalent to 79−81% per coupling−deprotection cycle). The relatively low yields are due to problematic coupling reactions connecting to the sterically demanding prolinol and valine residues, respectively. The carbamates at the *C*-terminus of **4**−**11** were formed in 60−73% yield. The preparation of the thiocarbamate **3** succeeded in only 20% yield. Deprotection and

RP-HPLC purification resulted in overall yields of 1−7% of isolated product for **4**−**11** and about 0.3% for **3**, respectively. All intermediates and the final products **3**−**11** were identified by MALDI-TOF MS. Compounds **4**−**11** were also fully characterized by 2D NMR spectra (TOCSY, ROESY, HSQC). All compounds were tested for their binding affinity to CD4 with SPR on a Biacore 3000 instrument, following the published procedure.[21,23] CD4 was immobilized on a CM5 chip, the activity of the immobilized CD4 was tested by determining the binding affinity of gp120. Subsequently, different concentrations of the ligands were passed over the surface to determine the concentration-dependent maximum response units (RU). The surface was regenerated with short pulses of 100 mM $H_3PO_4$. Only the lower concentrations (in general up to 50 $\mu$M) of the ligands resulted in data points fitting to a one-site binding model. Higher concentrations showed a nonsaturable linear correlation of concentration and response due to unspecific binding at higher concentrations. We observed this kind of behavior of peptide−protein interactions before.[21,23] It is either due to secondary binding sites of lower affinity on the protein or reflects the aggregation of peptides or peptidomimetics, respectively, at higher concentrations. As the peptidomimetics have different lipophilicity, aggregation starts at different ligand concentrations. Therefore, only data points following a one-site binding model at low concentrations of the ligand were used for the calculations of $K_D$ values. Examples for the fit of a one-site binding model to the data points from the SPR experiments are shown in Figure 1 for the compounds **4** and **5**. The concentration at $RU_{max}/2$ is $K_D$.

The binding affinities for **3**−**11** range from 6 $\mu$M (**4**) to 80 $\mu$M (**11**; see Table 1). The incorporation of new carboxy termini in **3**−**6** gave compounds with improved binding affinity compared to **2**. The binding affinities vary 2−6 times according to the carboxy terminal moiety relative to the most potent *tert*-butyl group. The comparison of the different carboxy terminal residues did not show a direct correlation between volume or molecular mass of the terminal group and the determined $K_D$. However, tertiary carbamates (compounds **4**, **7**−**9**, **11**) have generally higher binding affinities than secondary or primary carbamates (**2**, **3**, **5**, **6**, **10**). The directly corresponding compounds **4** and **7** and **8** and **9**, respectively, have varying aromatic amino terminal groups, the 2′-naphthyl oxycarbonyl (**4** and **9**) and 8′-quinolyl oxycarbonyl (**7** and **8**) residues, respectively. While **4** has a higher binding affinity to CD4 than **7**, **8** binds stronger to CD4 than **9**. This seemingly contradictory result shows that the binding affinities of the peptidomimetics cannot simply be calculated from a weighted contribution of each subunit, the influence of each subunit on the binding affinity is not linear. This would also explain why compounds **7**−**11**, which combine subunits that increase the binding affinity compared to **2**, do not have a drastically improved binding affinity. In fact, these findings match the later discussed modeling results, which show an influence of the carboxy terminus on the overall three-dimensional structure of the docked compounds. However, all compounds are still active binders of CD4. In the series of compounds synthesized in this paper, the prolinol subunit gives peptidomimetics with 3−6 times higher potency than the corresponding alaninol-containing compounds (comparing the compound pairs **4** and **9**, **7** and **8**, and **5** and **10**). This is a finding opposite to previous studies,[23] but is in accordance with our hypothesis about the importance of free-ligand conformation. The lipophilicity of the peptidomimetics (which is correlated to % acetonitril necessary to release the peptidomimetic from the RP-HPLC) is independent

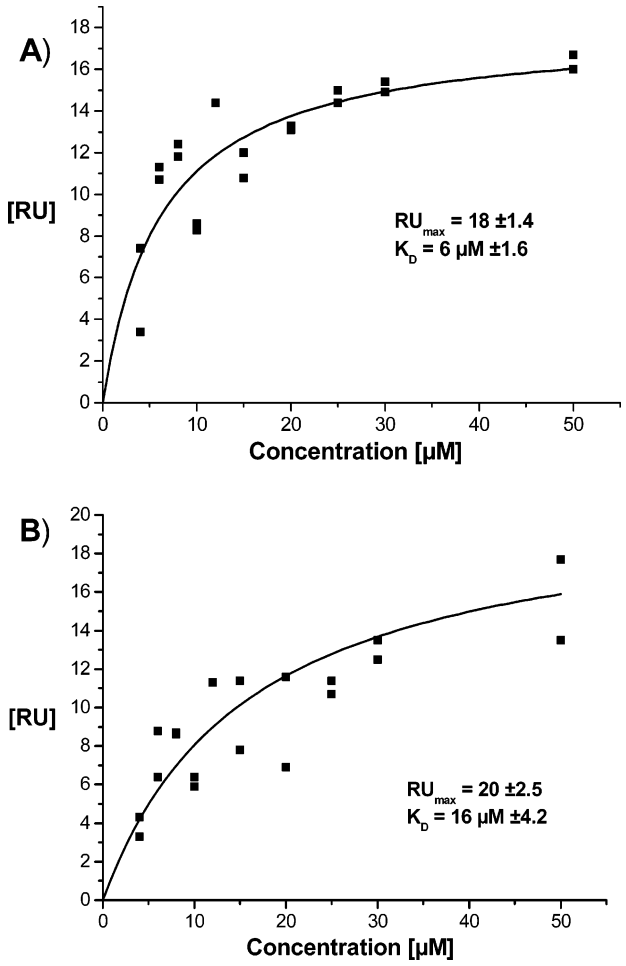


**Figure 1.** Determination of the binding constants of **4** (A) and **5** (B) by fitting the concentration-dependent RU values from a SPR experiment to a one-site binding model.

from the determined $K_D$ values. This indicates specific interactions rather than undefined hydrophobic interactions between the peptidomimetics and CD4.

Compounds **4** and **6** have been analyzed with STD NMR. Figure 2 shows the corresponding $^1$H NMR spectrums of a mixture of **4** and CD4 (top), the $^1$H NMR spectrum of **4** only (middle), and the $^1$H STD NMR spectrum of **4** binding to CD4 (bottom). The corresponding spectra of **6** are shown in the Supporting Information. The $^1$H STD NMR spectrum thereby shows only signals of the ligand **4**, with a change in intensity compared to the normal $^1$H NMR spectrum. The intensities of the signals in the STD NMR spectrum correlate not only to the number of protons, but also to the degree of saturation transfer and to the relaxation time of each individual proton. A high ratio of the integrals of the peaks in the $^1$H STD NMR spectrum to the integrals in the normal $^1$H NMR spectrum correspond to a high transfer of saturation (with disregard of the relaxation times). As the saturation transfer is a dipole−dipole interaction, a high degree of saturation transfer must be due to a close spatial contact between ligand and protein. The most prominent peaks in the $^1$H STD NMR, the protons of the aromatic ring, the Lys-H$\epsilon$ protons, the Val-H$\gamma$ protons, the ProH$\beta$/$\gamma$ protons, the Thr-H$\gamma$ protons, and parts of the carbamate (Figure 2) are, therefore, representative for the protons in close contact to CD4. This ligand epitope mapping derived from the STD NMR experiments of both compounds is depicted in Figure 3 by highlighting the respective protons in red. The ligand epitope of **4** and **6** is similar to each other and to previous findings.[21,23]

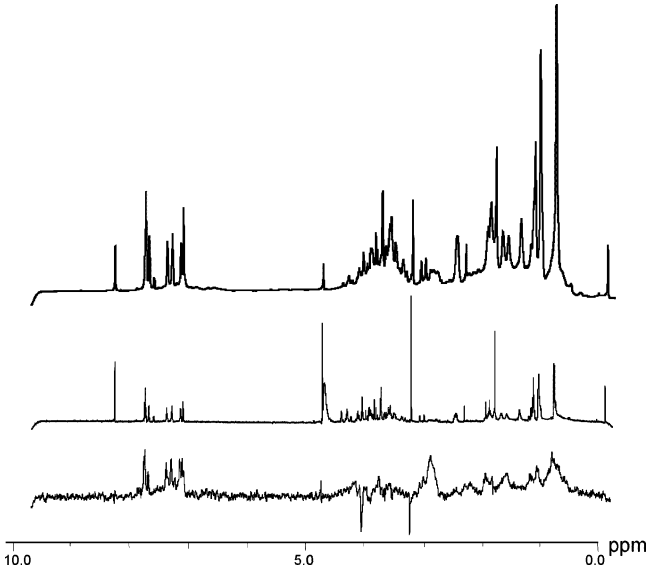


**Figure 2.** (top) $^1$H NMR spectrum of a mixture of **4** and CD4; (middle) $^1$H NMR spectrum of **4**; (bottom) $^1$H STD NMR spectrum of **4** when binding to CD4.

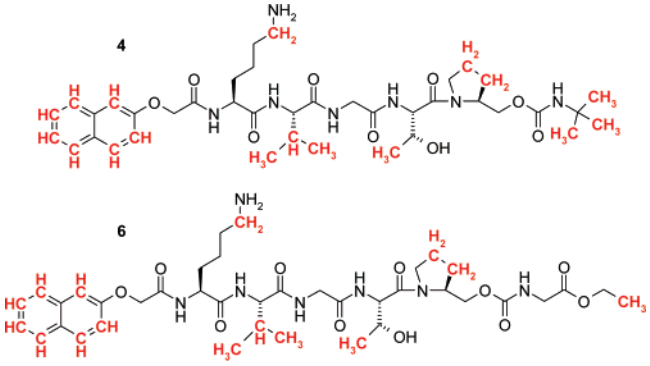


**Figure 3.** The binding epitopes of **4** and **6** determined by STD NMR. The protons highlighted in red are in close contact to CD4 (absolute STD NMR intensity of > 2.3% (**6**) and 1.7% (**4**), respectively).

STD NMR titration experiments provided information about the binding affinity of **4** and **6** to CD4 (Figure 4 and Tables 2 and 3). $^1$H STD NMR spectra of each compound were acquired at different ligand concentrations. A plot of the data points correlating the STD amplification factor and the ligand concentration can be fitted to a one-site binding model. This is done for individual protons. The $K_D$ values calculated by this method vary for different protons due to variances in the distance to CD4 and also slightly due to different relaxation times; both factors were not considered in the calculation of the individual $K_D$ values. The lowest determined $K_D$ value for a group of protons of one ligand is used for comparison with the $K_D$ values determined by SPR as earlier studies showed a good agreement for these $K_D$ values. The reason for this is that the group of protons with the lowest calculated $K_D$ value is in closest contact to CD4 and, thereby, gives the most accurate description of the binding affinity. The binding affinities of peptidomimetic **4** are $K_D = 6\ \mu M$ determined by SPR and $K_D = 16\ \mu M$ determined by STD NMR, while for compound **6** these values are $K_D = 37\ \mu M$ (STD NMR) and $K_D = 26\ \mu M$ (SPR), respectively. This is a very good overall agreement for the determination of binding constants by a homogeneous and heterogeneous system and lies well within experimental error. As both systems show compound **4** to be the better binder of CD4 than **6**, the ranking associated with the determined binding constants of all ligands in the SPR experiments is correct.

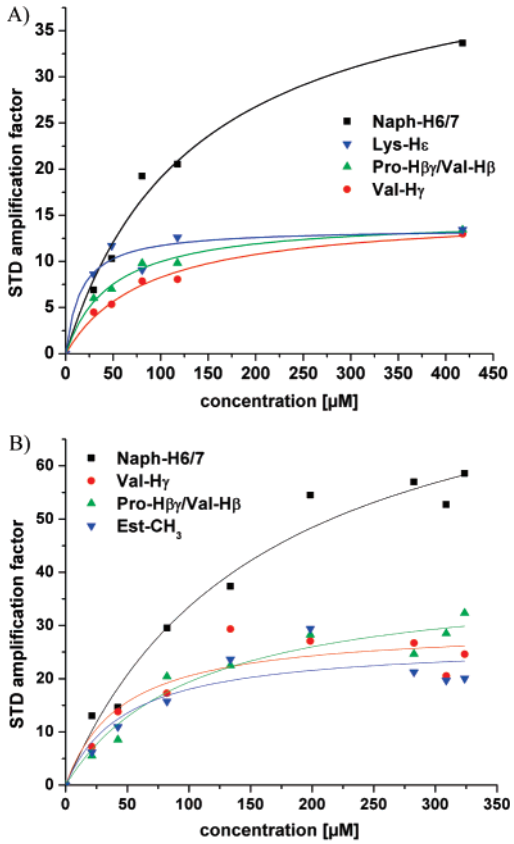


**Figure 4.** Determination of the $K_D$ values of **4** (A) and **6** (B) by fitting the concentration-dependent STD amplification factor to a one-site binding model.

**Table 2.** Individual $K_D$ Values for the Protons of **4** Determined from the STD NMR Experiment

| proton | individual $K_D$ value [mM] |
|---|---|
| naphthyl-H4/5/8 | 165 |
| naphthyl-H6/7 | 136 |
| naphthyl-H1/3 | 125 |
| Lys-H$\epsilon$ | 16 |
| Pro-H$\beta\gamma$/Val-H$\beta$ | 48 |
| *t*-Bu | 123 |
| Thr-H$\gamma$ | 88 |
| Val-H$\gamma$ | 86 |

**Table 3.** Individual $K_D$ Values for the Protons of **7** Determined from the STD NMR Experiment

| proton | individual $K_D$ value [mM] |
|---|---|
| naphthyl-H4/5/8 | 140 |
| naphthyl-H6/7 | 160 |
| naphthyl-H3 | 176 |
| naphthyl-H1 | 113 |
| Pro-H$\beta\gamma$/Val-H$\beta$ | 104 |
| Thr-H$\gamma$ | 37 |
| ester-$CH_3$ | 49 |
| Val-H$\gamma$ | 45 |

Compounds **2** and **6** were tested for their resistance to proteolysis by digesting them with pronase, adapting a method by Osapay et al.[25] The samples were incubated at 37 °C, and after 5, 10, 15, 20, and 30 min, aliquots of the reaction mixture were mixed with 1 M acetic acid to stop the digestion and

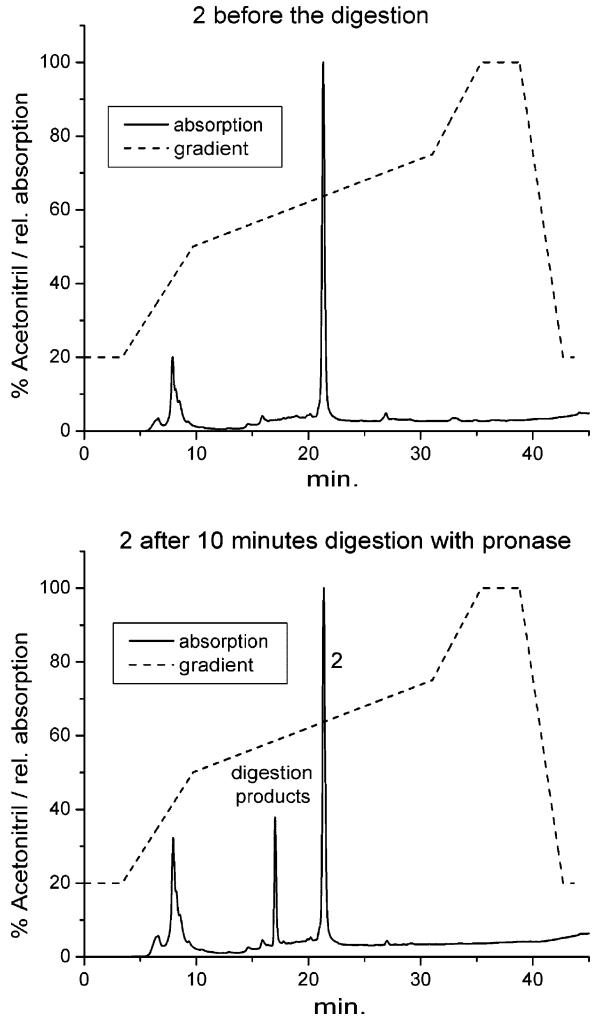


**Figure 5.** HPLC run of **2** prior to digestion (top) and after 10 min of digestion with pronase (bottom) at pH 7.5 and 37 °C.

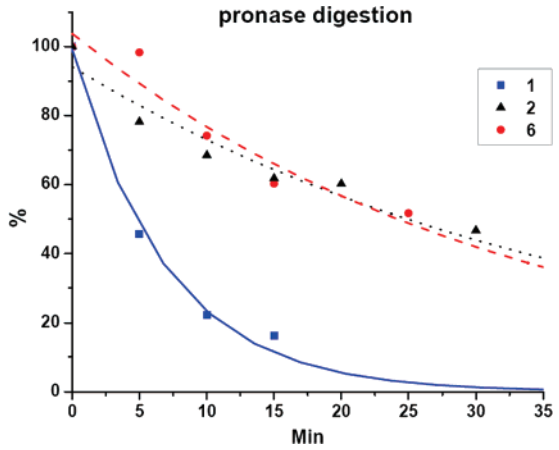


**Figure 6.** Comparison between the time-dependent proteolytic digestion of **1**, **2**, and **6**. The $t_{1/2}$ for the peptidomimetics **2** and **6** is roughly 4−5 times higher.

analyzed by HPLC-MS. Figure 5 shows the HPLC traces of **2** before the digestion and 10 min after the started digestion.

The integration of the peaks of the compounds **1**, **2**, and **6** at different times after the start of the digestion is represented in Figure 6 and allowed for the determination of $t_{1/2}$. The value of $t_{1/2}$ is 6 min for **1**, but is 27.3 min for **2** and 23 min for **6**, showing a much higher resistance to proteolytic digestion for the peptidomimetics than for a normal peptide.

**Table 4.** Hydrolysis Products Observed in the MALDI-TOF MS Spectra after the Digestion of **2** and **6** with Pronase[a]

| cmpd | exact mass [g/mol] | observed ions as $M + H^+/M + Na^+/M + K^+$ [*m*/*z*] |
|---|---|---|
| **2c** | 330.39 | 331/353/369 |
| **2d** | 483.61 | 484/506/522 |
| **2e** | 429.52 | 430/452/468 |
| **2f** | 384.48 | 385/407/423 |
| **2h** | 327.42 | 328/350/366 |
| **6b** | 615.73 | 616/638/654 |
| **6c** | 330.39 | 331/353/369 |
| **6e** | 429.52 | 430/452/468 |
| **6f** | 388.42 | 389/411/427 |
| **6h** | 331.37 | 332/354/370 |

[a] The mass of **6a** is too small to be detected in the MALDI-TOF MS.

The hydrolysis products of the digestion of **2** and **6** with pronase are not separated in the HPLC run, however, they have been analyzed by MALDI-TOF MS. The observed ions are summarized in Table 4. The digestion products result from the hydrolysis of the amide bonds between (2′-naphthyl)oxyacetic acid and lysine (only for **6**), lysine and valine, valine and glycine, and glycine and threonine (Figure 7). The threonine−prolinol amide bond and the carbamate bond were not hydrolyzed by pronase. Figure 7 shows the compounds **2** and **6**, respectively, and the cleavage sites to produce the observed ions.

Docking experiments were performed with Flexidock (Sybyl 6.9 (Tripos, Inc.) software package). A congruent binding mode for the compounds **3**−**11** is observed, which is also highly similar to the binding mode of similar compounds that has been described in detail before.[21,23] The highest degree of similarity is demonstrated for the interactions of the core peptides KVGTP and KVGTA, respectively (Figure 8). The lysine side chain has a close contact to the carboxylic side chain of $Asp_{63}$, the isopropyl group of valine is accommodated by a hydrophobic cavity formed by the side chains of $Trp_{62}$, $Ser_{42}$, $Phe_{43}$, $Arg_{59}$, $Ser_{60}$, and $Ser_{23}$, glycine does not exhibit any special interactions to the surface of CD4, and the threonine side chain interacts loosely with $Ser_{60}$. The docking experiment cannot explain the contacts of the proline $\beta$ and $\gamma$ protons with CD4, which was shown in the STD NMR experiments. The *N*- and *C*-termini of the docked compounds differ in the exact positions relative to the CD4. This is also true for compounds having the same terminal group, as, for example, is demonstrated for the compounds **4**, **7**, **8**, and **9** (different shades of magenta in Figure 8), which all share a *C*-terminal *tert*-butyl group. This corresponds to the finding that the binding affinity of the peptidomimetics cannot be calculated from individual contributions of each residue but also depends on the intramolecular interactions of the ligands. However, in all cases, the aromatic *N*-termini interact with $Gln_{40}$, $Gly_{41}$, and $Ser_{42}$.

The calculated binding affinity of compounds **2**−**11** was clearly better than that of the original peptide lead **1** (compare Table 1). The ranking of the compounds according to the calculated binding energies differs from the analytical findings. In Figure 9, the calculated binding energies of **1**−**11** and of related compounds of earlier reports[21,23] are plotted against the experimentally determined binding affinities.

Ideally, the logarithm of the $K_D$ values should correlate linearly with the calculated relative binding energy.[26] However, despite a positive correlation of the data, an $R^2$ value of 0.53 indicates that a direct calculation of binding affinities from the modeling data cannot be achieved in this way. A Spearman rank analysis of the correlation of modeling and analytical data,[27] which is independent of the distribution of the data points, gives

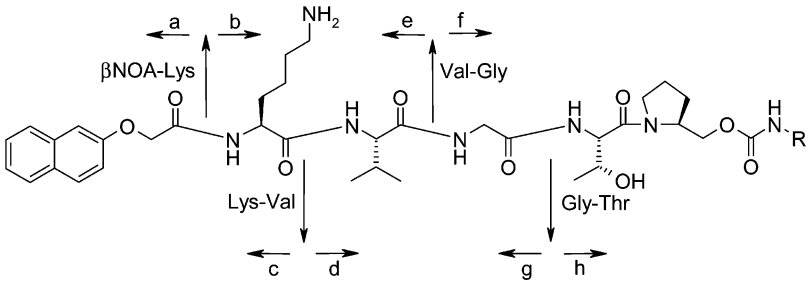


**Figure 7.** Digestion of the compounds **2** (R = cyclohexyl) and **6** (R = $CH_2CO_2Et$) with pronase resulted in the hydrolysis of the amide bonds between (2′-naphthyl)oxyacetic acid and lysine (only for **6**), lysine and valine, valine and glycine, and glycine and threonine. The observed hydrolysis products (named, e.g., **6e** for the carboxyl side after hydrolysis of the Val-Gly amide bond) are summarized in Table 4.

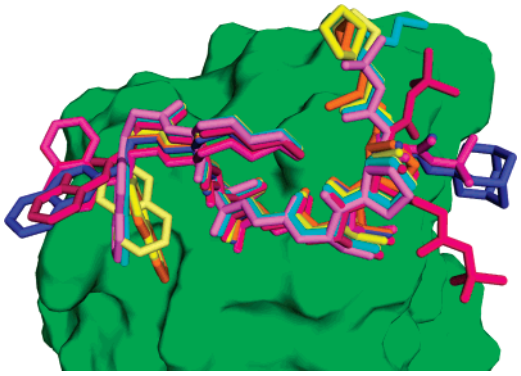

**Figure 8.** Overlay of the peptidomimetics **3** (orange), **4**, **7**, **8**, **9** (magentas), **6** (cyan), **5** and **10** (yellows), and **11** (blue) docked to CD4 (green surface). The core peptide KVGTP/A adopts a highly similar binding mode for all compounds, while the positioning of the termini differs.

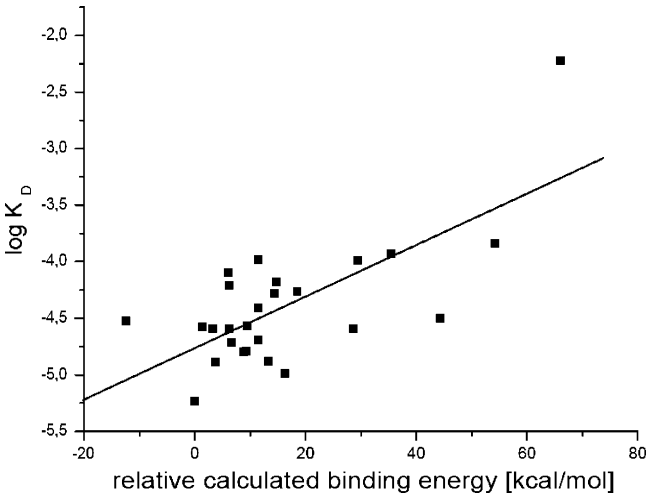


**Figure 9.** Plot of the data points for experimentally determined log $K_D$ values and the relative binding energies calculated with Flexidock. The relative binding energy of the compound with the highest binding affinity to CD4, i.e., **4**, was set to 0 kcal/mol.

a $R^2 = 0.61$. Both $R^2$ values are reasonable in comparison to other docking results.[28] In the modeling, all newly designed peptidomimetics presented here show better interaction with CD4 than **1**, and the peptidomimetics also have lower $K_D$s. The results are underlining the power of combining modeling and analytical data to direct the variation of known ligands to increase their binding affinity.

## Conclusion

The peptidomimetics developed in this paper bind strongly to CD4 and can, therefore, act as leads for potential HIV entry inhibitors. The best compound **4** has a $K_D = 6$ $\mu$M in the SPR experiments, which is 1000-fold better than the decapeptide lead **1** ($K_D = 6000$ $\mu$M). We, furthermore, could show a good agreement of the calculated binding energies with the experimentally determined binding affinities, as well as a reasonable agreement of the binding affinities determined by SPR and STD NMR. The STD NMR method not only supported the development of the peptidomimetics but was also used to prove binding affinity and verify the suggested binding mode. The pronase digestion showed a much higher proteolytic stability of the peptidomimetics compared to the lead peptide. The analysis of the digestion products furthermore underlined that the increased stability is due to the incorporated nonpeptide bonds.

## Experimental Section

**Synthesis:** The solid-phase syntheses were performed on an ACT 496-Ω robot system. 2′-Chlorotrityl resin (55 mg) bearing l-prolinol (50 mmol; ACT) was shaken for 2 h with Fmoc-Thr(tBu)-OH (4 equiv) and DIPEA/TBTU (5 equiv) in DMF. After washing the resin, this procedure was repeated twice. The resin was treated twice with 10% $Ac_2O$ in DMF for 15 min. Cleavage of the Fmoc group was achieved by treatment with 20% piperidine in DMF for 10 min twice. The next amino acids and 2-naphthoxy acetic acid were coupled by using the same protocol. The resin was transferred to a glass frit and was shaken with a freshly prepared solution of dichloromethane (1880 $\mu$L), TFA (20 $\mu$L), and TIPS (100 $\mu$L) for 1 h. The mixture was filtered, and the resin was then washed with the same solution (1 equiv) three times with dichloromethane. The combined solutions were washed three times with a 5% aqueous sodium acetate solution. The aqueous phase was re-extracted with dichloromethane, and the combined organic phases were shaken with Amberlyst A-21 for 1 h. The ion-exchange resin was filtrated and washed with dichloromethane, the organic phases were dried over $MgSO_4$, and the dichloromethane was evaporated to give the crude side-chain protected alcohols. The alcohols were each dissolved in dry DMF, and then a freshly prepared suspension of CuCl (50 mmol, 5 mg) in dry DMF (250 $\mu$L) and the respective iso(thio)cyanate (50 mmol) were added. This mixture was shaken for 1 h, then diluted with a 5% aqueous $(NH_4)HCO_3$ solution, and extracted three times with dichloromethane. The organic phase was dried over $MgSO_4$, and the solvents were evaporated to give the protected carbamates. These were individually dissolved in TFA (1.9 $\mu$L), TIPS (100 $\mu$L), and water (40 $\mu$L), and the solution was shaken for 1 h. The solvents were evaporated and the product was purified by HPLC (solvent A, water/acetonitrile (95:5); solvent B, water/acetonitrile (5:95); both solvents contained 0.1% TFA; gradient, 80% A for 1 column volume (CV), then gradients of 1 CV to 50% A and 5 CV to 0% A. Most products elute at two points from a preparative C18-substituted silica column, reflecting the elution of the protonated and the unprotonated form of the peptidomimetic. The identity of the products was demonstrated by MALDI-TOF and NMR spectra. The pure products were lyophilized to yield the final products **3**−**11**.

**Acknowledgment.** We thank the Deutsche Forschungsgemeinschaft (DFG) who supported this work with grants

through Graduiertenkolleg 464 and SFB 470/B2. We greatly acknowledge supply of CD4 from the AIDS reagent program.

**Supporting Information Available:** Purity of compounds, chemicals, characterization of the compounds **3**−**11**, including all NMR data and HPLC chromatograms or $^1$H NMR spectra, respectively, of **3**−**11**, the SPR graphs of **3** and **6**−**11** and details of the SPR and STD NMR experiments, the pronase digestion assay, and the docking procedure. This material is available free of charge via the Internet at http://pubs.acs.org.

## References


(1) Autran, B.; Carcelain, G.; Li, T. S.; Blanc, C.; Mathez, D.; Tubiana, R.; Katlama, C.; Debre, P.; Leibowitch, J. Positive effects of combined antiretroviral therapy on CD4+ T cell homeostasis and function in advanced HIV disease. *Science* **1997**, *277*, 112−116.

(2) (a) Squires, K. E. An introduction to nucleoside and nucleotide analogues. *Antiviral Ther.* **2001**, *6* (Suppl. 3), 1−14. (b) Ren, S.; Lien, E. J. Development of HIV protease inhibitors: A survey. *Prog. Drug Res.* **1998**, *51*, 1−31. (c) Bowers, M. Non-nucleoside reverse transcriptase inhibitors. *Bull. Exp. Treat. AIDS* **1996**, *Jun*, 19−22.

(3) Yang, Q. E. Eradication of HIV in infected patients: Some potential approaches. *Med. Sci. Monit.* **2004**, *10*, RA155−165.

(4) Tamalet, C.; Fantini, J.; Tourres, C.; Yahi, N. Resistance of HIV-1 to multiple antiretroviral drugs in France: A 6-year survey (1997−2002) based on an analysis of over 7000 genotypes. *AIDS* **2003**, *17*, 2383−2388.

(5) Kozal, M. Cross-resistance patterns among HIV protease inhibitors. *AIDS Patient Care Stand.* **2004**, *18*, 199−208.

(6) Lemckert, A. A.; Goudsmit, J.; Barouch, D. H. Challenges in the search for an HIV vaccine. *Eur. J. Epidemiol.* **2004**, *19*, 513−516.

(7) McMichael, A. J. HIV vaccines. *Annu. Rev. Immunol.* **2006**, *24*, 227−255.

(8) (a) Meadows, D. C.; Gervay-Hague, J. Current developments in HIV chemotherapy. *ChemMedChem* **2006**, *1*, 16−29. (b) Sticht, J.; Humbert, M.; Findlow, S.; Bodem, J.; Müller, B.; Dietrich, U.; Werner, J.; Kräusslich, H. G. A peptide inhibitor of HIV-1 assembly in vitro. *Nat. Struct. Mol. Biol.* **2005**, *12*, 671−677.

(9) Williams, I. G. Enfuvirtide (Fuzeon): The first fusion inhibitor. *Int. J. Clin. Pract.* **2003**, *57*, 890−897.

(10) Menzo, S.; Castagna, A.; Monachetti, A.; Hasson, H.; Danise, A.; Carini, E.; Bagnarelli, P.; Lazzarin, A.; Clementi, M. Genotype and phenotype patterns of human immunodeficiency virus type 1 resistance to enfuvirtide during long-term treatment. *Antimicrob. Agents Chemother.* **2004**, *48*, 3253−3259.

(11) (a) Dalgleish, A. G.; Beverly, P. C.; Clapham, P. R.; Crawford, D. H.; Greaves, M. F.; Weiss, R. A. The CD4 (T4) antigen is an essential component of the receptor for the AIDS retrovirus. *Nature* **1984**, *312*, 763−767. (b) Klatzmann, D.; Champagne, E.; Chemaret, S.; Gruest, J.; Guetard, D.; Hercend, T.; Gluckman, J. C.; Montagnier, L. T-lymphocyte T4 molecule behaves as the receptor for human retrovirus LAV. *Nature* **1984**, *312*, 767−768.

(12) (a) Sattentau, Q. J.; Moore, J. P.; Vignaux, F.; Traincard, F.; Poignard, P. Conformational changes induced in the envelope glycoproteins of the human and simian immunodeficiency viruses by soluble receptor binding. *J. Virol.* **1993**, *67*, 7383−7393. (b) Kwong, P. D.; Wyatt, R.; Robinson, J.; Sweet, R. W.; Sodroski, J.; Hendrickson, W. A. Structure of an HIV gp120 envelope glycoprotein in complex with the CD4 receptor and a neutralizing human antibody. *Nature* **1998**, *393*, 648−659.

(13) Bjorndal, A.; Deng, H.; Jansson, M.; Fiore, J. R.; Colognesi, C.; Karlsson, A.; Albert, J.; Scarlatti, G.; Littman, D. R.; Fenyo, E. M. Coreceptor usage of primary human immunodeficiency virus type 1 isolates varies according to biological phenotype. *J. Virol.* **1997**, *71*, 7478−7487.

(14) Bar, S.; Alizon, M. Role of the ectodomain of the gp41 transmembrane envelope protein of human immunodeficiency virus type 1 in late steps of the membrane fusion process. *J. Virol.* **2004**, *78*, 811−820.

(15) (a) Boussard, C.; Doyle, V. E.; Mahmood, N.; Klimkait, T.; Pritchard, M.; Gilbert, I. H. Design, synthesis and evaluation of peptide libraries as potential anti-HIV compounds, via inhibition of gp120/cell membrane interactions, using the gp120/CD4/Fab17 crystal structure. *Eur. J. Med. Chem.* **2002**, *37*, 883−890. (b) Vermeire, K.; Schols, D. Anti-HIV agents targeting the interaction of gp120 with the cellular CD4 receptor. *Exp. Opin. Invest. Drugs* **2005**, *14*, 1199−1212.

(16) (a) Biorn, A. C.; Cocklin, S.; Madani, N.; Si, Z.; Ivanovic, T.; Samanen, J.; Van, Ryk, D. I.; Pantophlet, R.; Burton, D. R.; Freire, E.; Sodroski, J.; Chaiken, I. M. Mode of Action for Linear Peptide Inhibitors of HIV-1 gp120 Interactions. *Biochemistry* **2004**, *24*, 1928−1938. (b) Schön, A.; Madani, N.; Klein, J. C.; Hubicki, A.; Ng, D.; Yang, X.; Smith, A. B., III. Thermodynamics of binding of a low-molecular-weight CD4 mimetic to HIV-1 gp120. *Biochemistry* **2006**, *45*, 10973−10980. (c) Ramurthy, S.; Lee, M. S.; Nakanishi, H.; Shen, R.; Kahn, M. Peptidomimetic antagonists designed to inhibit the binding of CD4 to HIV GP120. *Bioorg. Med. Chem.* **1994**, *2*, 1007−1013. (d) Allaway, G. P.; Davis-Bruno, K. L.; Beaudry, G. A.; Garcia, E. B.; Wong, E. L.; Ryder, A. M.; Hasel, K. W.; Gauduin, M. C.; Koup, R. A.; McDougal, J. S. Expression and characterization of CD4-IgG2, a novel heterotetramer that neutralizes primary HIV type 1 isolates. *AIDS Res. Hum. Retroviruses* **1995**, *11*, 533−539.

(17) Lifson, J. D.; Engleman, E. G. Role of CD4 in normal immunity and HIV infection. *Immunol. Rev.* **1989**, *109*, 93−117.

(18) Wang, J. H.; Meijers, R.; Xiong, Y.; Liu, J. H.; Sakihama, T.; Zhang, R.; Joachimiak, A.; Reinherz, E. L. Crystal structure of the human CD4 N-terminal two-domain fragment complexed to a class II MHC molecule. *Proc. Natl. Acad. Sci. U.S.A.* **2001**, *98*, 10799−10804.

(19) Myszka, D. G.; Sweet, R. W.; Hensley, P.; Brigham-Burke, M.; Kwong, P. D.; Hendrickson, W. A.; Wyatt, R.; Sodroski, J.; Doyle, M. L. Energetics of the HIV gp120-CD4 binding reaction. *Proc. Natl. Acac. Sci. U.S.A.* **2000**, *97*, 9026−9031.

(20) Wulfken, J. Development of CD4 binding peptides as inhibitors of HIV infection. Ph.D. Thesis, University of Hamburg, Germany, 2000.

(21) Neffe, A. T.; Meyer, B. A. peptidomimetic HIV-entry inhibitor directed against the CD4 binding site of the viral glycoprotein gp120. *Angew. Chem., Int. Ed.* **2004**, *43*, 2937−2940.

(22) (a) Mayer, M.; Meyer, B. Characterization of ligand binding by saturation transfer difference NMR spectroscopy. *Angew. Chem., Int. Ed.* **1999**, *38*, 1784−1788. (b) Mayer, M.; Meyer, B. Group epitope mapping by saturation transfer difference NMR to identify segments of a ligand in direct contact with a protein receptor. *J. Am. Chem. Soc.* **2001**, *123*, 6108−6117. (c) Meinecke, R.; Meyer, B. Determination of the binding specificity of an integral membrane protein by saturation transfer difference NMR: RGD peptide ligands binding to integrin $\alpha_{IIb}\beta_3$. *J. Med. Chem.* **2001**, *44*, 3059−3065. (d) Meyer, B.; Peters, T. NMR spectroscopy techniques for screening and identifying ligand binding to protein receptors. *Angew. Chem., Int. Ed.* **2003**, *42*, 864−890.

(23) Neffe, A. T.; Bilang, M.; Meyer, B. Synthesis and optimization of peptidomimetics as HIV entry inhibitors against the receptor protein CD4 using STD NMR and ligand docking. *Org. Biomol. Chem.* **2006**, *4*, 3259−3267.

(24) *Sybyl 6.5 Manual*; Tripos, Inc.: 1699 South Hanley Rd, St. Louis, MO, 1999.

(25) Osapay, G.; Prokai, L.; Kim, H. S.; Medzihradszky, K. F.; Coy, D. H.; Liapakis, G.; Reisine, T.; Melacini, G.; Zhu, Q.; Wang, H. S.; Mattern, R. H.; Goodman, M. Lanthionine-somatostatin analogs: Synthesis, characterization, biological activity, and enzymatic stability studies. *J. Med. Chem.* **1997**, *40*, 2241−2251.

(26) Neumann, D.; Kohlbacher, O.; Lenhof, H. P.; Lehr, C. M. Lectin-sugar interaction: Calculated versus experimental binding energies. *Eur. J. Biochem.* **2002**, *269*, 1518−1524.

(27) Lehmann, E. L.; D'Abrera, H. J. M. *Nonparametrics: Statistical Methods Based on Ranks*, revised ed.; Prentice Hall: Englewood Cliffs, NJ, 1998; pp 292, 300, and 323.

(28) Wang, R.; Lu, Y.; Wang, S. Comparative evaluation of 11 scoring functions for molecular docking. *J. Med. Chem.* **2003**, *46*, 2287−2303.


JM070206B